Tetrahedron Vol. 47, No. 14/15, pp. 2351-2364, 1991
Printed in Great Britain

0040-4020/91 $3.00+.00

Multisubstrate Adduct Inhibitors of Glycinamide Ribonucleotide Transformylase: Synthetic and Enzyme-Assembled.

James Inglese and Stephen J. Benkovic
Department of Chemistry, Pennsylvania State University, University Park, PA 16801

(*Received in USA* 27 *August* 1990)

Abstract: β-TGDDF, the displacement product of 2-thioacetamide ribonucleotide and N-10-(bromoacetyl)-5,8-dideazafolate, is a potent, slow, tight-binding, multisubstrate adduct inhibitor (MAI) of glycinamide ribonucleotide transformylase (GAR TFase; E.C. 2.1.2.2.). The mechanism of inhibition by this MAI and its derivatives are reported. In addition, a related series of MAIs formed from the interaction of glycinamide ribonucleotide (GAR) or its carbocyclic analog (carbo-β-GAR) and N-10-(bromoacetyl)-5,8-dideazafolate with GAR TFase have been discovered and characterized. These latter enzyme assembled inhibitors represent a novel route to the inhibition of GAR TFase.

Introduction

Glycinamide ribonucleotide transformylase (GAR TFase[1]; E. C. 2.1.2.2.) represents one of 18 known folate utilizing enzymes and is the first reduced-folate-requiring enzyme of *de novo* purine biosynthesis[2]. Although the major target of antifolates in the past has been dihydrofolate reductase (DHFR) (over 1,700 inhibitors as of 1984[3]) and to a lesser extent thymidylate synthase (TS)[4], interest in the development of antifolates aimed against the purine pathway transformylases has recently developed[5,6]. This pathway is an important target for anti-neoplastic agents[7] because of its role in providing purines for DNA synthesis, an important metabolic requirement in rapidly proliferating cells[8].

The concept of the multisubstrate adduct inhibitor, MAI[9,10], in the design of inhibitors of bimolecular or higher order enzyme catalyzed reactions has been successfully applied to the GAR TFase reaction[11]. GAR TFase catalyzes the one carbon transfer (at the oxidation state of formate) from the donor (6*R*,α*S*)-N10-formyl-tetrahydrofolate (N10-formyl-H_4F) to the amino group of β-glycinamide ribonucleotide (β-GAR). This transfer is believed to proceed via the tetrahedral intermediate shown in Figure 1, below which is shown the potent and specific MAI, β-TGDDF This adduct has a thermodynamic dissociation constant (K_D) on the order of 250 pM as determined by fluorescence titration binding and shows no significant affinity toward other reduced folate requiring enzymes, thus providing β-TGDDF with both high affinity and specificity .[11]

In this report we further describe the properties of β-TGDDF and related derivatives. For example, removal of the 5'-phosphoryl group from the adduct reduces the affinity of the inhibitor for GAR TFase by 7000-fold pointing to an important salt bridge interaction within the enzyme-inhibitor complex. A simple one-step binding mechanism for the interaction of β-TGDDF with enzyme is proposed based on the modeling of progress curves The off-rate of β-TGDDF from GAR TFase was determined to be on the order of 10^{-3} s^{-1} from trapping experiments utilizing a catalytically disabled mutant GAR TFase.

In addition, we have identified a novel MAI formed by the action of GAR TFase on its nbotide substrate, β-GAR, and the cofactor-based affinity label, N-10-(bromoacetyl)-DDF. This non-covalently bound MAI has been characterized and compared to β-TGDDF and exemplifies a rare type of inhibition whereby an enzyme catalyzes its own inhibition by generating at-site a tight-binding inhibitor and thereby providing a novel prototype for the design of drugs activated by metabolic assembly.

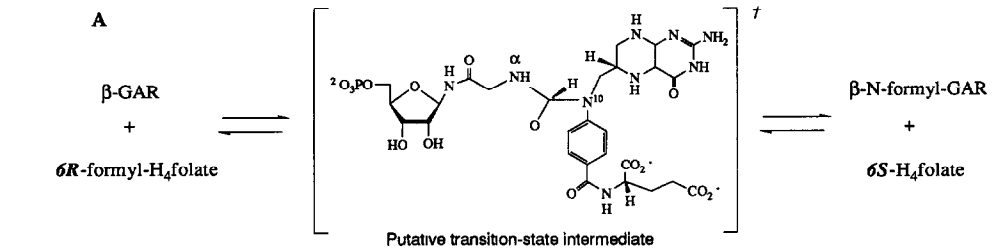

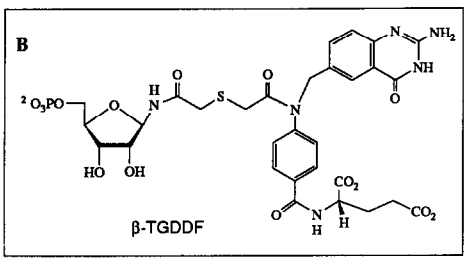

Figure 1: Reaction catalyzed by GAR TFase and the MAI, β-TGDDF. (**A**) Reaction of GAR TFase showing the proposed transition-state intermediate for the reaction. The tetrahedral hemiorthoamide transition state is believed to form by direct attack of the α-amino group of β-GAR onto the formyl carbon of the (6*R*, α*S*)-H4folate cofactor. (**B**) The MAI, β-TGDDF, is a stable bisubstrate adduct of the reaction components. Note that β-TGDDF, lacks elements of the putative hemiorthoamide tetrahedral carbon and, therefore by definition[9], is not a transition state analog.

Materials

All reagents were of the highest grade commercially available. Reagents for the synthesis of the inhibitor were purchased from Aldrich Chemical Co. Prostatic acid phosphatase, NADPH, dUMP, Tris, Hepes and A25-Sephadex were purchased from Sigma Chemical Co. 5,10-Methylene-tetrahydrofolate was prepared according to the method of Farina et al.[12] Tetrahydrofolate and *E. coli* DHFR were the kind gift of Joseph Adams, Penn State Univ *L casei* TS was the kind gift of Prof. D. V. Santi, UCSF. Mouse DHFR was the gift of Dr. Joell Thillet, Institute Jacques Monod, France. L1210 and HeLa GAR TFase were purified according to the procedure of Daubner & Benkovic.[13] AICAR TFase was prepared using the method of Mueller & Benkovic.[14] Plasmid-encoded wild type GAR TFase (D144 GAR TFase) from *E coli* was prepared according to Inglese et al.[15] and mutant GAR TFase (N144 GAR TFase) was prepared as described by Inglese et al.[16] Solutions of N-10-(bromoacetyl)-DDF used for enzyme catalyzed adduct formation were made in 50 mM Hepes, pH 7.5 [15] Glycinamide ribonucleotide (GAR) was prepared by the method of Chettur and Benkovic[17]; concentrations were determined enzymatically and represent the concentration of the β anomer (active anomer) The carbocyclic analogue of β-GAR was the gift of Dr. R. Vince, Department of Medicinal Chemistry, University of Minnesota

Experimental Procedures

General Methods

Continuous UV assays were recorded on a Beckman (Gilford) Model DUR recording quartz spectrophotometer or a Cary 219 spectrophotometer. UV spectra were recorded on a Perkin-Elmer Lambda Array 3840 UV/VIS spectrophotometer interfaced to a P&E 7300 PC. ^{1}H NMR were collected on a Bruker WB-360 spectrophotometer with chemical shifts being referenced versus the transmitter offset for HDO or $CHCl_3$ ^{31}P NMR were recorded on the same instrument using the heteronuclear probe with the transmitter offset referenced to trimethylphosphite. All proton spectra taken in D_2O were HDO

suppressed. Fluorescence spectra were recorded on an SLM Amico 8000C spectrophotometer

HPLC Methods. Stationary and Mobile Phases, and Gradients

HPLC was carried out on a Waters 600E with detection by a Waters 990 Photodiode Array Detector controlled by a NEC PowerMate 2 PC. HPLC columns used were as follows: Column A, Waters Delta Pak C-18 100 Å analytical column (3.9 mm x 30 cm); Column B, Perkin-Elmer C-18 0258-0148 analytical column (4.6 mm ID x 24.5 cm); Column C, Whatman Partisil 10 SAX column (4.6 mm ID x 25 cm, standard analytical); Column D, Whatman Partisil M9 10 / 50 ODS-3 semi-preparative column (50 cm x 9 mm ID). HPLC buffers and solvents were as follows: Buffer A, 0.01 M $NH_4H_2PO_4$, pH 3.5, 7% EtOH; Buffer B, 1 M $NH_4H_2PO_4$, pH 3.5, 7% EtOH; Solvent A, H_2O, 0.1% TFA; Solvent B, CH_3CN, 0.07% TFA.

Condition A. Reverse phase chromatography (column B; flow rate 1 ml/min; detection 230 nm) employing a gradient from 7% to 50% Solvent B over 50 min.

Condition B. Reverse phase chromatography (column B; flow rate 0.7 ml/min; detection 230 nm) using an isocratic system of 12% Solvent B

Condition C Anion exchange chromatography (column C; flow rate 1 ml/min; detection 238 nm) employing a 1% per min. linear gradient from 0% to 50% Buffer B.

Condition D. Reverse phase chromatography (column A; flow rate 1ml/min; detection 220-340 nm) employing a linear gradient from 0% Solvent B to 15% Solvent B over 60 min. followed by a 30 min. ramp to 70% solvent B.

Condition E. Reverse phase chromatography (column A; flowrate 1 ml/min.; detection 220-340 nm) employing a linear gradient from 0% Solvent B to 25% solvent B over 60 min.

Synthetic, Kinetic and Analytical Procedures

α,β-TGDDF The synthesis of α,β-TGDDF was accomplished as previously described.[11] The adduct was desalted on HPLC using condition A. Repurification using condition B [$t_r(\beta) \approx 31$ min., $t_r(\alpha) \approx 35$ min.] gave pure single anomers of the adduct. The solution of pure anomer must be neutralized (aqueous NH_3) before concentration (Speed-Vac), since in the presence of TFA, anomerization occurs. An approximately equimolar mixture of α- and β-anomers resulted as judged by HPLC and ^1H NMR. The adduct has been obtained in yields ranging from 50% to 100% when a five-fold excess of thioGAR was employed. Often during the coupling reaction a side product, N-10-(hydroxyacetyl)-DDF forms which is poorly resolved from α-TGDDF as shown in Figure 2. The alcohol can be removed from the α,β mixture by anion exchange chromatography (condition C; t_r(alcohol) ≈ 12 min., $t_r(\alpha, \beta) \approx 24$ min.) and then the anomers can be separated from one another as outlined above

^1H NMR spectrum of the anomeric mixture (D_2O): δ 7.7-7.5 (m, 3 , p-phenylene and H-5), δ 7.42 (t, 1, H-7), δ 7.2-7.14 (m, 3, *p*-phenylene and H-8), δ 5.44 (d, 1, $J_{H1'-H2'}$ = 4.4 Hz, α-anomeric C1'-H), δ 5.24 (d, 1, $J_{H1'-H2'}$ = 5.3 Hz, β-anomeric C1'-H), δ 4.87 (s, 2, C9-CH_2), δ 4 36 (m, 1, glutamic acid C_α-H), δ 4.2-3.7 (4, C5'-CH_2, C3'-CH, C2'-CH), δ 3 21 (m, 4, CH_2SCH_2), δ 2.16 (t, 2, $J_{\beta-\gamma}$=7.4 Hz, glutamic acid C_γ-H), δ 1.95 (two multiplets, 2, glutamic acid C_β-H). UV (50 mM Hepes, pH=7.5): λ_{max} 230 (ε = 54.5 $cm^{-1}mM^{-1}$), λ_{sh} 255 (ε = 26.1$cm^{-1}mM^{-1}$), λ_{max} 310 (ε = 4 19 $cm^{-1}mM^{-1}$)

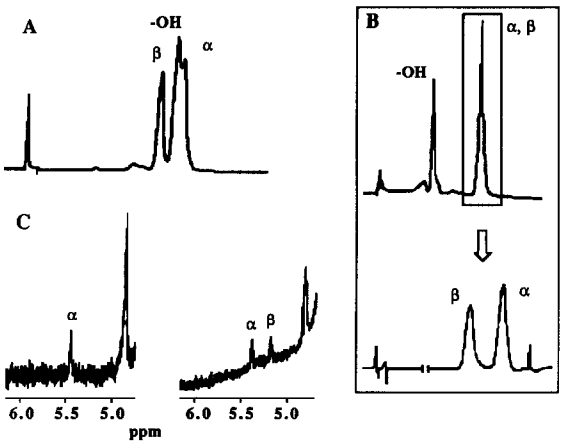

Figure 2: Resolution and stereochemical assignment of α- and β-TGDDF anomers. (A) The α- and β-TGDDF anomers can be resolved using C18 reverse phase HPLC. Unremoved HOAcDDF (-OH), a by-product of the coupling reaction, elutes close to the α anomer and can be removed prior to the reverse phase step by anion exchange chromatography (B). (C, left) ^{1}H NMR of the anomeric proton region of the second HPLC peak from the lower right reverse phase HPLC chromatogram. (C, right) ^{1}H NMR of an equal mixture of both HPLC peaks. The downfield shift and smaller $J_{H1'-H2'}$ value of the proton from the isolated anomer relative to the other C1' proton signal (from the mixture) is characteristic of a ribose substituted at C1' in the α position[24]. The identification of the first and second eluting peaks are therefore β- and α-TGDDF, respectively.

Enzymatic Synthesis of α,β-TGDDF Riboside To 40 µl of a 50 µM solution of α,β-TGDDF buffered to pH 4.0 with 20 mM sodium acetate was added 4 µl of prostatic acid phosphatase (1mg lyophilized enzyme / 1ml H_2O). The reaction was allowed to stir 2 hrs. at 22°C after which time the solution was injected onto either an anion exchange or a reverse phase HPLC system, using conditions C or A, respectively.

Steady-State Kinetics. All GAR TFase assays were conducted at 26°C in 50 mM Hepes, 0.5 mM EDTA, pH 8.4. The folate analog N-10-formyl-DDF was used as the formyl donor and the reaction was monitored at 295 nm ($\Delta\varepsilon$ = 18.9 mM^{-1} cm^{-1}). Depending on the particular assay the reaction was started with either enzyme (full time course) or GAR (initial rate analysis). When reactions were begun with GAR, the enzyme was allowed to incubate with substrates and inhibitor for 10-15 minutes prior to addition of GAR. Reactions volumes were either 1 or 0.5 ml and concentrations of substrates were 30 µM β-GAR and 40 µM N-10-formyl-DDF unless stated otherwise.

Specificity studies Experiments were carried out by incubating 1 nM of the respective enzyme with 20 nM β-TGDDF for 5 min. The reaction was initiated by adding saturating quantities of substrates. Transformylase reactions were monitored at 295 nm using N-10-formyl-DDF as the cofactor for the GAR TFase reaction and N-10-formyl-8-deazafolate as the cofactor for the AICAR TFase reaction. The DHFR reactions were monitored at 340 nm which corresponds to NADPH turnover. The thymidylate synthase reaction was monitored at 338 nm corresponding to dihydrofolate formation. All reactions were conducted at 26°C in a volume of 1 ml of the appropriate buffer. Assay details for appropriate enzymes can be found in: (a) avian GAR TFase[18], (b) HeLa O & L1210 GAR TFase[13], (c) avian AICAR TFase[14], (d) *E coli* DHFR[19], (e) mouse DHFR[20] and (f) *L casei* TS[4].

Fluorescence Titrations Fluorescence titrations of the MAIs; α- , β-TGDDF, GADDF, and CGADDF with GAR TFase were carried out using the general procedure described in Inglese et al.[11]

Off-rate Determination. Wild type GAR TFase (0 5 nM) was incubated for 10 min. with 3 equivalents of β-TGDDF (enough β-TGDDF to cause complete inhibition) in 50 mM Hepes, 0 5 mM EDTA, pH 8.5. To this solution was added a solution of substrates (final concentrations were 24 µM β-GAR and 40 µM N-10-formyl-DDF or 100 µM β-GAR and 100

μM N-10-formyl-DDF) and N144 GAR TFase (final concentration was 110 nM). The reaction time course was recorded by monitoring DDF formation. The data was fit to equation 1 which describes an exponential increase limited by a linear phase.

$$f(x) = t[m(1-e^{-kt})] \quad \text{(eqn. 1)}$$

where t is time in seconds, m is the slope of the linear phase, and k is the rate constant for the exponential process.

Computer Simulations. Kinetic models were simulated and compared to steady-state data using the program Simul[21] as modified to accept data as x,y pairs[22]. Fast equilibrium was assumed for all substrate and product binding events. The kinetic parameters for *E. coli* GAR TFase were used: $k_{cat} \approx 40$ sec^{-1}, N-10-formyl-DDF $K_m = 36$ μM, GAR $K_m = 24$ μM.[15] Morrison's type A and B slow tight-binding inhibition mechanisms were used as models. Experimental progress curves were fit to both mechanisms by varying the on and off rates for mechanism A, or the pre-equilibrium constant and the rates for forward and reverse isomerization for mechanism B.[23]

Dissociation constants and off-rate data were fit to hyperbolic and exponential-linear functions, respectively, using the program RS1 (BBN software Products Corp.)

Identification of Enzyme Generated MAIs (GADDF and CGADDF) HPLC (condition D) was used to identify new folate containing components. Hydrolysis products of N-10-(bromoacetyl)-DDF were injected and their points of elution and UV spectra recorded. A solution of 26 μM D144 GAR TFase, 370 μM β-GAR or β-carbo-GAR and 34 μM N-10-(bromoacetyl)-DDF was incubated at 22°C for 12 hrs. then analyzed by HPLC. A control in which 50 mM Hepes (pH 7 5, 0.5 mM EDTA) replaced enzyme was also analyzed. In all experiments described in this study N-10-(bromoacetyl)-DDF was added last and after all other components were incubated at the prescribed temperature for 10 min.

Time Course of Enzyme Catalyzed GADDF Formation via D144 and N144 GAR TFase The time course for the formation of the MAI was obtained by incubating 50 mM Hepes buffer (pH 7.5, 0.5 mM EDTA), 16 μM D144 GAR TFase or 16 μM N144 GAR TFase, 500 μM β-GAR (α,β mixture), 44 μM N-10-(bromoacetyl)-DDF at 22°C. Aliquots of 41 μl were removed, quenched with 1μl of concentrated TFA and frozen (liquid nitrogen) at appropriate times. Components were analyzed by HPLC (Condition E) using the 254 nm absorbance for quantification. Peak areas were converted to concentrations by having the sum of the peak areas of the N-10-(bromoacetyl)-DDF and MAI peak equal 44 μM. The stoichiometry of GADDF formation was also extracted from this experiment.

Stoichiometry of Enzyme Catalyzed GADDF Formation Product (GADDF) stoichiometry was determined by two separate experiments. The first is described above and the second is described here. Solutions of 50 mM Hepes (pH 7 5, 0.5 mM EDTA), 10.3 μM D144 GAR TFase, 390 μM β-GAR (α,β mixture) and 2.6-20.6 μM N-10-(bromoacetyl)-DDF at 22°C were incubated for 12 hrs. A control in which no enzyme was added was also done. Components were quantitated by HPLC (condition E) using the 254 nm absorbance and peak areas were converted into concentrations as described above.

Acid Phosphatase Assay of Enzyme Generated MAIs (GADDF and CGADDF) To a 10 μl solution of 130 μM MAI in 10 mM HCl (pH 3.5) was added 1 μl of a 1 mg/ml solution of prostatic acid phosphatase (prepared using distilled water). Following a 2 hr incubation period at 22°C the solution was injected onto the HPLC (condition C) and products were observed with decreased retention times similar to those found upon dephosphorylation of α, β-TGDDF.

Amino Acid Analysis. Degradation of MAI's for amino acid analysis was carried out under vapor phase acid hydrolysis conditions (constant boiling HCl at 165°C for 45 min. in a sealed Teflon bomb). Amino acid derivatizations were performed on an Applied Biosystems Model 420A Derivatizer and the PTC derivatives analyzed on a Model 120A Analyzer.

Results and Discussion

β-TGDDF and Derivatives

The synthesis of β-TGDDF has been described elsewhere[11], but briefly the adduct was constructed in a regiospecific fashion by employing the nucleophilic GAR analog, 2-thioacetamide ribonucleotide or ThioGAR (based on the methodology of Schendel & Stubbe[24]) and the electrophilic affinity reagent, N10-(bromoacetyl)-DDF[25]. The mixture of α and β anomers (resulting from epimerization at C1' of the ribose moiety) could be separated and their configurations established by proton NMR (Figure 2).

β-TGDDF appears to be enzyme specific for GAR TFase but apparently not species specific, inhibiting the transformylase from *E coli*[11,15,16], avian[18], HeLa O[13], and murine L1210[13] sources and displaying a slow, tight-binding inhibition pattern. Other folate requiring enzymes tested were dihydrofolate reductase (DHFR) from *E coli* [19]and mouse[20], and thymidylate synthase (TS) from *L casei*[4]. Neither of these enzymes were inhibited by β-TGDDF. Interestingly, aminoimidazolecarboxamide ribonucleotide transformylase (AICAR TFase) from chicken liver is also not inhibited by β-TGDDF at concentrations causing total inhibition of GAR TFase. This, however, may not be surprising in light of the fact that, in addition to unique ribotide specificities, the deazafolate specificity for GAR TFase and AICAR TFase are different .[26]

α-TGDDF Analysis of the β anomer showed it to posses a dissociation constant of 250 ± 50 pM[11] when measured using a modification of the fluorescence titration method of Taira and Benkovic[27]. By contrast, the α anomer was less potent, but surprisingly by only a factor of 20-fold (Table 1). Modeling studies in which both α and β anomers are conformationally constrained at the deazafolate and phosphate groups, then minimized reveal an energy difference of ≈ 2 kcals (20-fold) between them.[28] This computational analysis agrees with the experimental difference in dissociation constants and suggests that the thiomethylene tether between the binding determinants (folate and phosphate) can allow the opposite anomer of GAR enough degrees of freedom to bind with only a marginal loss in affinity.

Effects of Removing the 5'-Phosphoryl Group The importance of the phosphate group to binding is dramatically shown upon its hydrolysis by acid phosphatase. As shown in Table 1, high affinity binding is lost when the non-phosphorylated derivative of TGDDF is tested as an inhibitor of *E coli* GAR TFase. When compared to β-TGDDF a ≈7000-fold decrease in binding can be directly attributed to removal of the phosphate. This derivative has a K_I similar to dideazafolate (DDF) itself indicating that the remainder of the ribosyl moiety contributes little toward binding affinity and is probably more critical in conferring specificity.

Mechanism of Inhibition by β-TGDDF As shown in Table 2, both anomers of TGDDF act as slow, tight-binding inhibitors of *E coli* GAR TFase as evident from the relatively slow onset of inhibition and the low concentration of inhibitor ($[I_t] \approx [E_t]$) required to cause this inhibition. A representative set of progress curves for the inhibition of *E coli* GAR TFase in the presence of varying quantities of β-TGDDF is shown in Figure 3a. This

pattern of curves in which the initial rate of the reactions appears to be independent of inhibitor concentration suggests that inhibition follows the simpler of two general mechanisms proposed by Morrison[23] to describe this type of inhibition, mechanism A (Figure 3b). The other mechanism (mechanism B, Figure 3b) contains an isomerization step ($E \cdot I \rightleftharpoons E \cdot I^*$) subsequent to formation of the E·I complex. Such a mechanism is often characterized by a pattern of progress curves where the initial rates are dependent on inhibitor concentration.

Table 1. Binding constants for folate analogs with *E coli* GAR TFase.

Compound	$K_D(\mu M)^{\dagger}$	$K_I(\mu M)^{\S}$	$K_m(\mu M)^{\S}$
10-formyl-DDF	-	-	36
β-GAR	-	-	23
DDF	-	28.1	-
β-TGDDF	2.5x10-4	-	-
α-TGDDF	5.8x10-3	-	-
α, β-TGDDF riboside	-	1.7	-
GADDF	$2.5x10^{-4}$	-	-
CGADDF	$1.1x10^{-4}$	-	-

†Determined using fluorescence titrations as described under Experimental Procedures. Concentrations of inhibitors and enzymes used in titrations were: [β-TGDDF] = 11 nM, enzyme stock = 0.95 μM; [α-TGDDF]= 126 nM, enzyme stock = 60 μM. [GADDF & CGADDF] = 9 nM, enzyme stock = 1 μM Error ± 20%. §Determined as described in ref. 15. Error ± 20%.

Table 2. Classification of inhibitor type*

Inhibitor	$[I_t]$ (nM)	$[I_t]/[E_t]$	$t_{1/2}^{\dagger}$	Inhibition type§
α, β-TGDDF riboside	4000	5,970	rapid‡	classical
5,8-dideazafolate	51,000	76,120	rapid‡	classical
β-TGDDF#	2.3	3.5	≈2.6 min	slow, tight
α-TGDDF	25.2	37.6	≈2 8 min	slow, tight

*The [GAR TFase] = 0.67 nM, [CHO-DDF] = 25.5 μM and [GAR(β)] = 146 μM for the assays. §Defined according to ref. 23. †The onset of steady-state rate. ‡Not observable on the min.-sec. time scale. #GADDF and CGADDF gave similar results.

Although there appears to be no dependence of initial rate on [I], a computer simulation provides a fit of these data to either mechanism A or B (Figure 3). For mechanism A, a dissociation constant of 250 pM was obtained which could be factored into an on-rate, $k_{on} = 4 \cdot 10^6\ M^{-1}sec^{-1}$, and off-rate, $k_{off} = 1 \cdot 10^{-3}\ sec^{-1}$.[29,30] When a model was constructed according to mechanism B inhibition (pre-equilibration of a loose complex between substrate and inhibitor followed by isomerization to a tighter complex), the data would be fitted by the model if a dissociation constant of 15 μM for the pre-equilibrium was used. The overall dissociation constant, however,

remains the same as that for the simpler mechanism. But to show the effect of inhibitor on the initial rates, an extremely high concentration of inhibitor would be required, making measurement of the rates impossible so that mechanism B cannot be unequivocally ruled out. It would appear, however, that under the conditions used for our experiments mechanism A can appropriately describe the binding of β-TGDDF to *E coli* GAR TFase without the need to invoke the more complex process described by mechanism B.

Off-Rate of β-TGDDF From the E·β-TGDDF Complex The k_{off} of β-TGDDF from the enzyme·inhibitor complex (E·I*) was directly measured through a trapping experiment described by equation 2.

$$E{\cdot}I^* \underset{k_{on}}{\overset{k_{off}}{\rightleftharpoons}} E + I \xrightarrow{[E']\,k'_{on}} E'{\cdot}I + E \qquad \text{(eqn 2)}$$

where E is wild type GAR TFase, E' is N144 GAR TFase, I is β-TGDDF, k_{off} is the dissociation rate of I from E, k_{on} is the second-order formation rate constant for wild type GAR TFase and I, and k_{on}' is the second-order formation rate constant for N144 GAR TFase and I. The appearance of active E was monitored by following the

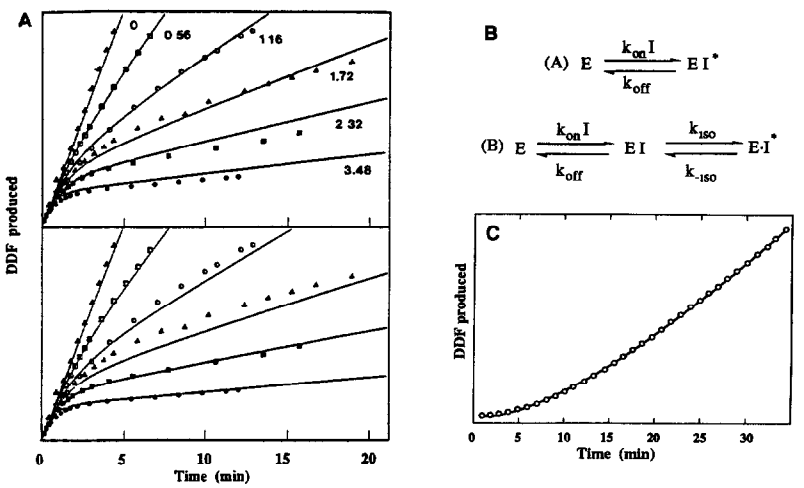

Figure 3: Progress curves and modeling of the inhibition of GAR TFase by β-TGDDF. (**A**) Progress curves and KINSIM analysis for slow, tight-binding inhibition of *E coli* GAR TFase by β-TGDDF. [Enzyme] = 1 nM and inhibitor concentrations are given (in nM) in the figure. Symbols are experimental data and solid lines are computer fits as defined by either mechanism A (**A**, top) or mechanism B (**A**, bottom) as described in text. (**B**) Description of mechanisms A and B, Mechanism A represents a simple one-step binding process and mechanism B represents a two-step process in which the second step describes an isomerization defined by the rate constants k_{iso} and k_{-iso}. This second step can represent a slow enzyme isomerization, the slow displacement of bound solvent molecules or perhaps an inhibitor isomerization. (**C**) Off-rate trapping experiment. The progress curve shows the increase in enzyme activity as β-TGDDF dissociates from the E β-TGDDF complex and becomes trapped by excess inactive N144 GAR TFase. The rate of increase in enzyme activity, as measured by DDF produced, is equal to the off-rate (k_{off}) of the inhibitor and is expected to follow an exponential function.

formation of DDF from the 10-formyl DDF and α,β GAR present in the solution. In this experiment it is assumed the inhibitor off-rate reflects the increase in the rate of DDF formation with time (d[DDF] / dt). The data was approximated by an exponential increase followed by a linear phase whose slope is proportional to the rate of turnover of free E providing an estimate of $k_{off} \cong 0.0014 \pm 0.0008\ s^{-1}$ (representative data is given in Figure 3d). This value is close to the estimate from steady-state experiments[30] and the computer simulations (Figure 3a).

Enzyme Catalyzed Bisubstrate Adduct Formation

Kinetics. In the absence of GAR (glycinamide ribonucleotide) the transformylase is irreversibly inactivated by N10-(bromoacetyl)-DDF[15, 25] as demonstrated by the time and concentration dependent loss in activity shown in Figure 4 (solid lines). The site of covalent modification between affinity label and enzyme was determined in the *E coli* transformylase to be aspartic acid 144[16]. The presence of DDF affords protection against the effects of the alkylating reagent so the Asp 144 is probably at the active site If GAR TFase is preincubated with GAR before the addition of the affinity label apparent partial inhibition (Fig 4, dotted line) is observed. It was subsequently shown (Figure 5a) that there was no covalent attachment to the enzyme by N10-(bromoacetyl)-DDF in this case. Instead it is possible to isolate by HPLC a stoichiometric amount of a new material having chemical and biological properties very similar to β-TGDDF. Figure 5b shows that the production of this adduct by GAR TFase is maximized at a ratio of 1:1 of N10-(bromoacetyl)-DDF to GAR TFase (in the presence of excess GAR)

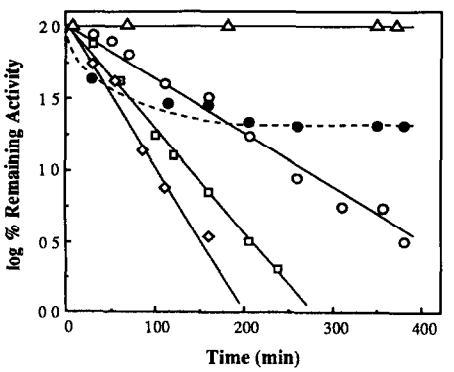

Figure 4: Plot of log (% GAR TFase activity remaining) vs. time for various concentrations of DDF and GAR in the presence of 330 μM N10-(bromoacetyl)-DDF (△) no inhibitor, no DDF, (○) 1.6 mM DDF, (□) 0.223 mM DDF, (◇) 0 mM DDF, (●) 0 mM DDF, 1.3 mM β-GAR.

Structural Characterization of New Inhibitors We have demonstrated by several lines of analysis that this material is a bisubstrate adduct formed from the incubation of N10-(bromoacetyl)-DDF and GAR in the presence of GAR TFase. Interestingly the carbocyclic analogue of GAR, carbo-GAR, also forms a binary E·S complex capable of undergoing MAI formation. The carbo- GAR analogue has previously been shown to be a substrate for the transformylase reaction from mammalian and bacterial sources employing either the natural cofactor, N10-formyl-H_4F, or the quinazoline cofactor, N10-formyl-DDF[31, 15].

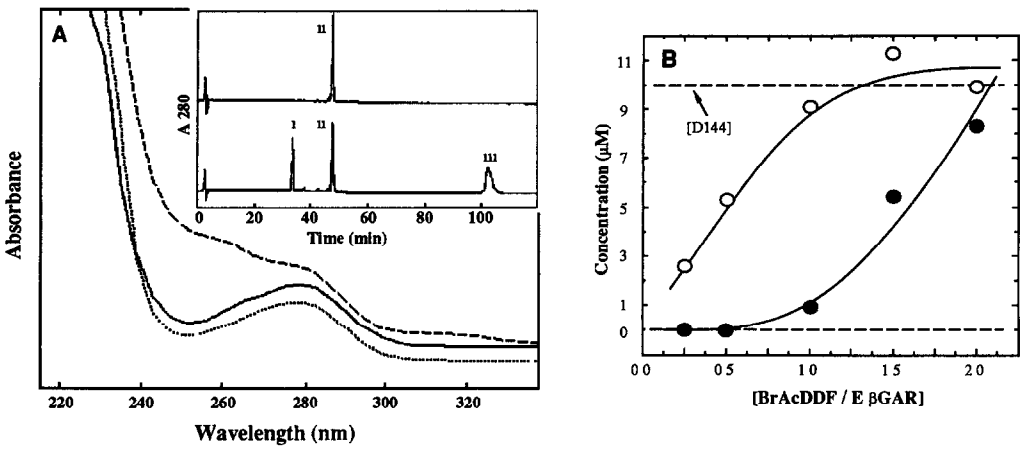

Figure 5: Identification and Stoichiometry of formation of new inhibitor. (A) UV spectra of GAR TFase species. (- - -) GAR TFase covalently labeled with 1 equivalent of N10-(bromoacetyl)-DDF, (——) GAR TFase used to catalyze bisubstrate formation and separated from adduct by HPLC and (------) untreated GAR TFase The untreated GAR TFase spectrum has been displaced for clarity and all spectra represent equal concentrations of enzyme. (inset) Reverse phase HPLC analysis of reaction mixture used to generate bisubstrate adducts. (top) GAR and N10-(bromoacetyl)-DDF (II) incubated at 37°C without enzyme and (bottom) incubation in the presence of GAR TFase (III). The MAI (GADDF) is peak I. (B) Titration of GAR TFase-β-GAR with N10-(bromoacetyl)-DDF. (●) [N10-(bromoacetyl)-DDF remaining after 12 hrs. and (○) [GADDF] formed after 12 hrs. Analysis was accomplished by HPLC as described in text.

The structures of the new inhibitors, termed here glycinamide ribonucleotide acetyl 5,8-dideazafolate (GADDF) and carbocyclic glycinamide ribonucleotide 5,8-dideazafolate (CGADDF), were inferred from the components of the

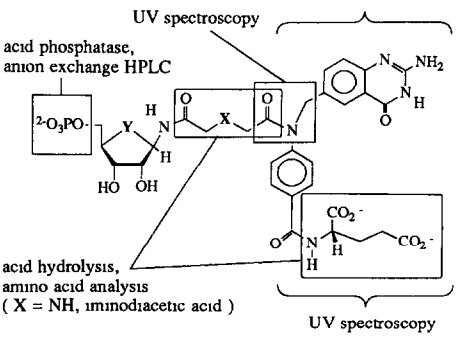

Figure 6: Structures and analysis methods of the phosphoribosyldideazafolate MAIs formed by GAR TFase Glycinamide ribonucleotide acetyl dideazafolate (GADDF; Y = O, X = NH) and carbocyclic glycinamide ribonucleotide acetyl dideazafolate (CGADDF; Y = CH_2, X = NH). The presence of the molecular substructures (boxed and bracketed regions) were confirmed by the analysis method indicated. β-TGDDF (Y = O, X = S).

reaction and confirmed by spectroscopic and enzymatic analysis (Figure 6). The MAIs were identified as new early eluting peaks on HPLC (Figure 5a, inset) containing the N10-substituted chromophore. Phosphatase treatment of GADDF and CGADDF followed by analysis on anion exchange HPLC indicated, by their elution at shorter retention times, a phosphate ester was associated with these molecules attesting to the presence of the GAR moiety

When acid hydrosylates of GADDF and CGADDF were examined by amino acid analysis the presence of iminodiacetic acid was observed indicating the nature of the linkage between the folate and ribose molecules to be the secondary amine indicated in Figure 6.

In addition both GADDF and CGADDF gave similar inhibition patterns and dissociation constants as those observed for β-TGDDF (Table 1 & 2) when tested as inhibitors of *E coli* GAR TFase. Of further interest is the observation of the formation of the adduct by the site-specific mutant GAR TFase, D144N. In this mutant the residue Asp 144, believed to be the critical base in catalysis has been replaced by asparagine resulting in a protein capable of binding substrates and inhibitors but unable to carry out the formyl transfer reaction.[16] The formation of GADDF occurs at the same rate under the conditions described when either wild type (D144) GAR TFase or the catalytically compromised N144 GAR TFase mutant (binding intact) is employed thus indicating the enzyme is simply acting as a binding pocket for reaction components. A fit of this data (Figure 7) to a single exponential gave a rate of formation of $k_{MAI} = 0.089 \pm 0.011$ min^{-1} ($t_{1/2} = 7.7$ min)[32]. This MAI assembly capability reflects the catalytically compromised transformylase's ability to still properly bind and correctly position the nucleophilic primary amine group of GAR within bonding distance of the electrophilic bromoacetyl group of N10-(bromoacetyl)-DDF which presumably must be juxtaposed in a manner similar to the substrates in the normal reaction [16]

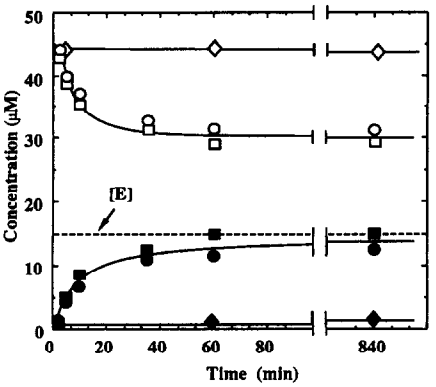

Figure 7: Time course for the formation of GADDF as catalyzed by GAR TFase. (□) [N10-(bromoacetyl)-DDF], (■) [GADDF] as catalyzed by D144 GAR TFase and (○) [N-10-(bromoacetyl)-DDF], (●) [GADDF] as catalyzed by N144 GAR TFase. The dotted line represents the enzyme concentration. (◇) [N10-(bromoacetyl)-DDF] and (◆) [GADDF] in the absence of GAR TFase (see Ref. 32). Analysis was accomplished by HPLC (condition E) as described in text.

Conclusion

β-TGDDF and GADDF (& CGADDF) represent a new class of GAR TFase inhibitors. These phosphoribosylfolates combine a phosphoribosyl moiety and folate analog by a 6-atom linker arm that joins the folate at N10 to the ribose at C1'. Linker arms bridged by either sulfur or nitrogen display similar properties. Adducts devoid of the 5'-phosphate are incapable of high affinity binding implying that the ribose appendage alone offers little toward the establishment of the tight enzyme-inhibitor complex.

Some potential uses of this new class of GAR TFase inhibitor include: competition traps to aid in obtaining individual rate constants for the elementary steps in the transformylase mechanism much as MTX was applied in the elucidation of the kinetic mechanism of DHFR[33]; as ligands for the x-ray crystallographic study of *E coli* GAR TFase[34] which should enable the identification of relevant residues involved in substrate and cofactor recognition; and as a proto-drug for the design of selective inhibitors of GAR TFase.

The observation that the substrate GAR appears to "protect" GAR TFase from inactivation by N10-(bromoacetyl)-DDF provides an interesting example of an enzyme catalyzed synthesis of an MAI. This finding suggests that the reactive bromoacetyl group of the affinity label may overlap with the amino group of GAR at the active site; certainly a reasonable assumption if formyl transfer proceeds by the intermediacy of a tetrahedral adduct shown in Figure 1. This type of adduct formation is not unique, a similar situation was observed by Chase and Tubbs[35] in the case of the inactivation of carnitine acetyltransferase by the carnitine ester of bromoacetate and coenzyme A. The enzyme was observed to be rapidly inactivated by the formation of a noncovalently bound multisubstrate adduct at the active site when incubated with the bromoacetate ester and coenzyme.

The nonlinear plot obtained for the log %R activity vs. time shown in Figure 4 can be rationalized in terms of an enzyme catalyzed inhibition process generating a slowly dissociating noncovalent E·I complex An inhibition profile of this type was reported by Manderschied and Wild[36] for the inhibition of *Triticum aestivum* L. glutamine synthetase by phosphinothricin. Inhibitors of enzymes acting by this assembly process may provide a means of fabricating complex structures (e.g., MAIs) within cells themselves from simpler components. Such a form of drug delivery would be useful because in some cases potentially useful enzyme inhibitors cannot penetrate the cell membrane in their active form often due to their charged nature. The transport problem has alternatively been addressed in several different and clever ways, for example, by using transportable esters[37] to be later processed by esterases, or neutral species that become charged after undergoing an enzyme catalyzed redox process[38]; or alternatively improving inhibitor transport via liposomes[39]. Rideout [40] has suggested the idea of generating cytotoxins in cells by the self-assembly of individual components. This process, however, does not require the intermediacy of a target enzyme but rather the non-enzymatic coupling of non-toxic molecules to generate a cytotoxic substance and takes advantage of the steeper dose-response relationship and sensitivity to concentration of a simultaneous two molecule therapy relative to responses utilizing individual molecules.

In addition to the observation of a novel form of inhibition, the MAI formation process has aided in addressing some questions about the probable mechanism of GAR TFase. The N144 mutant, although unable to catalyze formyl transfer, can catalyze MAI synthesis. This establishes that N144 GAR TFase retains the capacity to bind both ribotide and folate substrates The D144N mutation appears to uncouple acid / base and entropic catalysis and serves to illustrate the importance of catalytic residues in the GAR TFase reaction; an entropy trap alone is insufficient to catalyze formyl transfer but completely sufficient to catalyze MAI formation.

The work presented here demonstrates that potent and specific inhibitors for this enzyme can be made using a rational approach based on mechanistic and structural information Two specific types of inhibitors have been

described which have similar properties, the pre-made MAI, β-TGDDF and the in situ derived MAIs, GADDF and CGADDF. Studies aimed at characterizing and evaluating these new compounds have increased our understanding of the transformylase reactions as well as defined structural components and geometries required for the development of specific and potent inhibitors of this enzyme.

Notes and References

This study was supported by grants from the National Institutes of Health to S.J.B. (GM24129). J. I. is the recipient of a Homer Braddock Research Fellowship; present address: Howard Hughes Medical Institute, Duke University Medical Center, Durham NC 27710.

1. Abbreviations: β-TGDDF, β-thioglycinamide ribonucleotide 5,8-dideazafolate; DHFR, dihydrofolate reductase; TS, thymidylate synthase; MAI, multisubstrate adduct inhibitor, GAR TFase (also D144 GAR TFase), glycinamide ribonucleotide transformylase; N10-(bromoacetyl)-DDF, N10-(bromoacetyl)-5,8-dideazafolate; GADDF, glycinamide ribonucleotide acetyl 5,8-dideazafolate; CGADDF, carbocyclic glycinamide ribonucleotide acetyl 5,8-dideazafolate; DDF, 5,8-dideazafolate; CHO-DDF, N10-formyl-5,8-dideazafolate; β-GAR, β-glycinamide ribonucleotide; N144 GAR TFase, a catalytically inactive mutant GAR TFase in which the amino acid residue aspartate 144 has been replaced by asparagine 144 (see ref. 16).
2. For a reviews see: Inglese, J.; Johnson, D. L.; Benkovic, S J. In *Chemistry and Biology of Pteridines, Proceedings of the 9th International Symposium*; Curtius, H -Ch., Ghisla, N., Blau, N., Eds ; deGruyter: Berlin, 1990; pp 951-956 and references therein.
3. Blaney, M. B.; Hansch, C.; Silipo, C., Vittoria, A. *Chem Rev* **1984,** *84*, 333-407.
4. Santi, D. V.; Danenberg, P. V. In *Folates and Pterins 1*, Blakley, R. L., Benkovic, S. J., Eds; John Wiley & Sons: New York, 1984; Chapter 9.
5. Chabner, B. A.; Allegra, C. J.; Baram, J. In *Chemistry and Biology of Pteridines, Proceedings of the 8th International Symposium*; Cooper, B. A., Whitehead, V. M., Eds ; deGruyter: Berlin, 1986; 945-957.
6. Beardsley, G P.; Moroson, B. A.; Taylor, E. C.; Moran, R G. *J Biol Chem.* **1989,** *264*, 328-333.
7. Elion, G. B. *Science* **1989,** *244*, 41-47.
8. Hitchings, G. H ; Elion, G. B.; Falco, E. A.; Russell, P. B ; Sherwood, M. B.; Vanderwerff, H. *J. Biol Chem* **1950,** *183*, 1-9.
9. Broom, A. D. *J Med Chem* **1989,** *32*, 2-7.
10. Wolfenden, R.; Frick, L. In *Enzyme Mechanisms*, Page, M. I., Williams, A., Eds.; Royal Society of Chemistry: London, 1987; pp 97-122.
11. Inglese, J.; Blatchley, R. A.; Benkovic, S J. *J Med Chem.* **1989,** *32*, 937-940.
12 Farina, P. F.; Farina, L S.; Benkovic, S J. *J Am Chem Soc.* **1973,** 5409-5411.
13. Daubner, S.C. & Benkovic, S.J. *Cancer Res* **1985,** *45*, 4990-4997
14. Mueller, W T.; Benkovic, S. J. *Biochemistry* **1981,** *20*, 337-344.
15 Inglese, J.; Johnson, D. L.; Shiau, A., Smith, J. M.; Benkovic, S. J. *Biochemistry* **1990,** *29*, 1436-1443.
16. Inglese, J.; Smith, J M.; Benkovic, S. J. *Biochemistry* **1990,** *29*, 6678-6687.
17. Chettur, C. A.; Benkovic, S. J. *Carbohydr Res* **1977,** *56*, 75-86
18. Young, M.; Sammons, R. D.; Mueller, W. T.; Benkovic, S. J. *Biochemistry* **1984,** *23*, 3979-3986.
19. Baccanari, D.; Phillips, A.; Smith, S , Sinski; Burchall, J. *Biochemistry* **1975,***14*, 5267-5273.
20 Thillet, J., Absil, J.; Stone, S. R.; Pictet, R *J. Biol Chem* **1988,** *263*, 12500-12508.
21. Barshop, B. A., Wrenn, R. F.; Frieden, C. *Anal Biochemistry* **1983,** *130*, 134-145.
22. Anderson, K. S.; Sikorski, J. A., Johnson, K. A. *Biochemistry* **1987,** *90*, 7395-7406.
23. Morrison, J. F ; Walsh, C T. *Adv Enzymol Relat Areas Mol Biol* **1987,** *57*, 201-301.
24. Schendel, F. J.; Stubbe, J *Biochemistry* **1986,** *25*, 2255-2264.
25. Daubner, S. C.; Young, M.; Sammons, R D.; Courtney, L. F.; Benkovic, S. J. *Biochemistry* **1986,** *25*, 2951-2957.
26 Smith, G. K.; Mueller, W. T.; Benkovic, P. A., Benkovic, S J *Biochemistry* **1981,** *20*, 1241-245
27. Taira, K.; Benkovic, S. J. *J Med Chem* **1988,** *31*, 129-137.
28. MM2 energy minimizations were accomplished on an Evans & Sutherland PS390 graphics system using the subroutine MULTIFIT (used to preform a flexible fit between two or more molecules) from the Sybyl 5.0 / Mendyl 1 2 (1987) molecular modeling program

29. Capperelli (1989) determined the mechanism for lymphoma L5178Y GAR TFase to be ordered-sequential with the cofactor binding first. The on-rate of the first substrate in an ordered-sequential mechanism is equal to the k_{cat}/K_m [Dalziel, K. *Acta Chem. Scand.*, **1957**, *11*, 1706.]. For L5178Y GAR TFase this value for the DDF cofactor is $k_{on} = 3.3 \times 10^6\ M^{-1}\ s^{-1}$ and for *E coli* GAR TFase is $k_{on} = 1.1 \times 10^6\ M^{-1}\ s^{-1}$ (based on the values from ref. 15.).
30. After a solution 1 nM in both enzyme and β-TGDDF was incubated for 10 min., sufficient GAR was added to produce a 100 mM solution, and the fluorescence intensity at 395 nm (excitation at 275) was monitored over time. Simple exponential curve fitting on the data suggests a k_{off} of $<0.007\ s^{-1}$ with approximately 25% of the complex dissociating[10].
31. Caperelli, C. A.; Price, M. A. *Arch. Biochem Biophys.* **1988**, *264*, 340-342.
32. After 4 days approximately 2% MAI was formed as judged by HPLC from a mixture of β-GAR and N10-(bromoacetyl)-DDF at concentrations equal to those used in the presence of GAR TFase, 500 μM and 44 μM, respectively. From these data a rough estimate of the rate enhancement for the enzyme would be approximately 10^4.
33. Fierke, C. A.; Johnson, K. A.; Benkovic, S. J. *Biochemistry* **1987**, *26*, 4085-4092.
34. Stura, E.; Johnson, D.L.; Inglese, J.; Smith, J M.; Benkovic, S.J.; Wilson I.A. *J Biol Chem* **1989**, *264*, 9703-9706.
35. Chase, J F A.; Tubbs, P K. *Biochem J* **1969**, *111*, 225-235
36 Manderscheid, R.; Wild, A. *J Plant Physiol* **1986**, *123*, 135-142
37. Nogrady, T. In *Medicinal Chemistry A Biochemical Approach*, 2nd Ed.; Oxford University Press: New York, 1988.
38. Bodor, N.; Farag, H. H.; Brewster, M. E. *Science* **1981**, *214*, 1370
39. Bangham, A. D. In *Liposomes from Physical Structure to Therapeutic Applications*, Knight, G , Ed.; Elsevier North-Holland: New York, 1981.
40. Rideout, D. *Science* **1986**, *233*, 561-563.